Biochemical and Biophysical Research Communications 425 (2012) 456–461

Contents lists available at SciVerse ScienceDirect

Biochemical and Biophysical Research Communications

journal homepage: www.elsevier.com/locate/ybbrc

Phosphorylation of Na–Cl cotransporter by OSR1 and SPAK kinases regulates its ubiquitination

Muhammad Zakir Hossain Khan, Eisei Sohara *, Akihito Ohta, Motoko Chiga, Yuichi Inoue, Kiyoshi Isobe, Mai Wakabayashi, Katsuyuki Oi, Tatemitsu Rai, Sei Sasaki, Shinichi Uchida

Department of Nephrology, Graduate School of Medicine, Tokyo Medical and Dental University, 1-5-45 Yushima, Bunkyo-ku, Tokyo 113-8519, Japan

ARTICLE INFO

Article history:
Received 11 July 2012
Available online 27 July 2012

Keywords:
Na–Cl cotransporter
Phosphorylation
Ubiquitination
Pseudohypoaldosteronism type II
Dietary salt

ABSTRACT

Na–Cl cotransporter (NCC) is phosphorylated in its amino terminus based on salt intake under the regulation of the WNK-OSR1/SPAK kinase cascade. We have observed that total protein abundance of NCC and its apical membrane expression varies in the kidney based on the phosphorylation status. To clarify the mechanism, we examined NCC ubiquitination status in mice fed low, normal and high salt diets, as well as in a model mouse of pseudohypoaldosteronism type II (PHAII) where NCC phosphorylation is constitutively elevated. Low-salt diet decreased NCC ubiquitination, while high-salt diet increased NCC ubiquitination in the kidney, and this was inversely correlated with total and phosphorylated NCC abundance. In the PHAII model, the ubiquitination of NCC in kidney was also lower when compared to that in wild-type littermates. To evaluate the relationship between phosphorylation and ubiquitination of NCC, we expressed wild-type, phospho-deficient and -mimicking NCC in COS7 cells, and the ubiquitination of immunoprecipitated total and biotinylated surface NCC was evaluated. NCC ubiquitination was increased in the phospho-deficient NCC and decreased in phospho-mimicking NCC in both total and surface NCC. Thus, we demonstrated that NCC phosphorylation decreased NCC ubiquitination, which may contribute to the increase of NCC abundance mostly on plasma membranes.

1. Introduction

The thiazide-sensitive NaCl cotransporter (NCC) is essential for sodium reabsorption at the distal convoluted tubules (DCT) in the kidney. A loss-of-function NCC mutation causes Gitelman's syndrome, an inherited disease that exhibits salt-losing phenotypes [1]. In contrast, a gain-of-function mutation in NCC causes pseudohypoaldosteronism type II (PHAII), a disease of salt-sensitive hypertension. PHAII was shown to be caused by mutations in the with-no-lysine kinases 1 and 4 (WNK1 and WNK4) [2], and we clarified using a PHAII model mouse (*Wnk4*$^{D561A/+}$) that the pathogenesis of PHAII was the constitutive activation of a phosphorylation signal cascade consisting of WNK kinase, oxidative stress-responsive kinase-1 (OSR1), STE20/SPS1-related proline/alanine-rich kinase (SPAK), and NCC [3].

NCC is phosphorylated at several amino-terminal serine and threonine residues (T53, T58 and S71 in mouse NCC) by OSR1/SPAK [4], which is highly elevated in *Wnk4*$^{D561A/+}$ knock-in mice [3]. SPAK knockout mice showed decreased phosphorylation of NCC at these sites and exhibit Gitelman's syndrome-like phenotypes [5], thus confirming the importance of NCC phosphorylation in the *in vivo* function of NCC. Pacheco-Arevarez et al. showed that the phosphorylation of NCC is important for its transport function when expressed in *Xenopus* oocytes [6]. In addition to this mechanism, it was observed that phosphorylated NCC was concentrated on the plasma membranes of DCT, thus suggesting that phosphorylation is involved in the accumulation of NCC in plasma membranes [7,8].

We recently reported several physiological regulators of NCC phosphorylation. NCC phosphorylation is increased by a low-salt diet through aldosterone [9]. Angiotensin II and insulin were found to increase NCC phosphorylation [10–13]. Interestingly, total protein abundance of NCC appeared to vary according to NCC phosphorylation in these cases. Similar phenomena were also observed in *Wnk4*$^{D561A/+}$ knock-in, SPAK knockout, SPAK and OSR1 knock-in mice [3,5,14], thus suggesting that NCC phosphorylation is able to regulate its total protein abundance mostly on plasma membranes. However, the underlying mechanisms of how phosphorylation of NCC increases surface expression have yet to be clarified.

Numerous membranous proteins, including various ion transporters of the kidney, have been shown to be degraded in a regulated manner that involves ubiquitination. For example, epithelial sodium channel (ENaC) is ubiquitinated by Nedd4-2, and ubiquitinated ENaC is sorted to a degradation pathway [15]. Impaired ENaC ubiquitination at the cell surface by the mutation of ENaC in Liddle

* Corresponding author. Fax: +81 3 5803 5215.
E-mail address: esohara.kid@tmd.ac.jp (E. Sohara).

0006-291X/$ - see front matter © 2012 Elsevier Inc. All rights reserved.
http://dx.doi.org/10.1016/j.bbrc.2012.07.124

syndrome results in increased ENaC protein levels at the cell surface, leading to increased sodium reabsorption and hypertension [16,17]. In the case of NCC, it has been reported that NCC is polyubiquitinated in its secretory pathway (ER) and undergoes proteasomal degradation [18]. It has also been reported that ubiquitin ligase Nedd4-2 ubiquitinates NCC [19]. These observations suggest that NCC phosphorylation and ubiquitination are coordinated and involved in the regulation of NCC under various pathophysiological conditions.

In this study, we found that dietary salt intake regulates NCC ubiquitination and phosphorylation *in vivo*. Similarly, NCC ubiquitination was decreased in a PHAII mouse model. In addition, we clarified that NCC phosphorylation regulates NCC ubiquitination. Thus, ubiquitination of NCC may be an important determinant of NCC protein abundance and plasma membrane localization within cells.

2. Materials and methods

2.1. Animal study

C57BL/6 mice (age, 12 weeks) were fed normal diet, low-NaCl diet (0.01% NaCl (w/w)) or high-NaCl diet (4% NaCl (w/w)) for 14 days. *Wnk4*$^{+/+}$ and *Wnk4*$^{D561A/+}$ mice were fed normal diet. All animal procedures were approved by the Institutional Animal Care and Use Committee of the Tokyo Medical and Dental University.

2.2. Immunoprecipitation of NCC from mouse kidney

Mice were sacrificed after 14 days on the diet. Whole kidneys were homogenized in homogenization buffer (250 mM sucrose, 10 mM triethanolamine, 1 mM EGTA, 1 mM EDTA, 20 mM *N*-ethylmaleimide (NEM), 50 mM sodium fluoride, 1 mM sodium orthovanadate and complete protease inhibitor). Isolated crude membrane fraction (17,000*g*) was solubilized in buffer SB (0.5% sodium-deoxycholate, 20 mM Tris HCl, 5 mM EDTA, 10% glycerol and complete protease inhibitor). Samples were precleared by incubating with immobilized protein G, and were then subjected to NCC immunoprecipitation by rabbit anti-NCC antibody (Chemicon, Temecula, CA, USA). As a negative control, samples were incubated with rabbit IgG.

2.3. Plasmids

Full-length wild-type T7-tagged NCC and T7-tagged phospho-deficient NCC expression plasmid (pRK5-T7-tagged NCC and pRK5-T7-tagged NCC) was kindly provided by Dr. T. Moriguchi [20]. T7-tagged phospho-mimicking NCC (pRK5-T7-tagged NCC) was generated by site-directed mutagenesis with using the QuikChange Mutagenesis system (Stratagene, La Jolla, CA, USA).

2.4. Cell culture and transient transfection

COS7 cells were grown in low bicarbonate Dulbecco's modified Eagle's medium supplemented with 10% (v/v) fetal calf serum. Cells were transfected with 8 μg of each plasmid using Lipofectamine 2000 (Invitrogen, CA, USA).

2.5. Immunoprecipitation of transiently expressed NCC in COS7 cell

Empty vector (PRK-5), T7-tagged phospho-deficient, wild-type or phospho-mimicking NCC was transfected into COS7 cells. At 48 h after transfection, cells were lysed with buffer M-PER (Thermo Scientific, Massachusetts, USA) containing 20 mM NEM and complete protease inhibitor. Lysates were centrifuged at 17,000*g* for 30 min. Supernatant was precleared with immobilized protein G, and was then subjected to NCC immunoprecipitation by rabbit anti-NCC antibody bound to protein A-Sepharose beads.

2.6. Cell surface biotinylation assay

COS7 cells were transfected with empty vector (PRK-5), T7-tagged phospho-deficient, wild-type or phospho-mimicking NCC. Cell surface proteins were labeled with sulfo-NHS (*N*-hydroxysuccinimido)-SS-biotin (Thermo Scientific) at 48 h after transfection as follows: cells were washed three times with PBS-CM (PBS with 1 mM $MgCl_2$ and $CaCl_2$). Cells were incubated for 30 min on ice with 0.5 mg/ml sulfo-NHS-SS-biotin in PBS-CM, and were then quenched with 100 mM glycine in PBS-CM. After washing three times with PBS-CM, cells were lysed in buffer M-PER (Thermo Scientific) containing 20 mM NEM and complete protease inhibitor. Lysates were centrifuged at 17,000*g* for 30 min. For pull down of total surface protein, lysates were incubated with immobilized NeutrAvidin beads (Pierce) at 4 °C for 2 h. For pull down of cell surface NCC, lysates were precleared with immobilized protein G, and were then subjected to the NCC immunoprecipitation by rabbit anti-NCC antibody (Chemicon, Temecula, CA, USA). NCC immune complexes bound to the protein A-Sepharose beads were eluted by boiling for 15 min in 100 μl of 1% SDS in PBS (pH 7.2) and diluted with 900 μl of PBS (pH 7.2). The solution was then incubated for 1 h at 4 °C with immobilized NeutrAvidin beads (Thermo Scientific) to isolate the biotinylated NCC surface fraction.

2.7. Immunoblotting

Semi-quantitative immunoblotting was performed, as described previously [21,22]. To assess relative expression levels of proteins in whole kidney, homogenates without the nuclear fraction (600*g*) or the crude membrane fraction (17,000*g*) were used. Band intensity was analyzed using Image J (NIH, Betheda, MD, USA). To quantify ubiquitinated protein signals from immunoblots, we calculated the amount of protein (in arbitrary units) from a 6-fold dilution series of the same protein that was also immunoblotted. The following primary antibodies were used in this study: rabbit total anti-NCC [23]; guinea pig total anti-NCC [23]; rabbit anti-pNCC (T53, T58 and S71) [9]; anti-T7 (from Invitrogen); and mouse anti-ubiquitin (Santa Cruz Biotechnology, CA, USA). Alkaline-phosphatase-conjugated anti-IgG antibodies (Promega, Madison, WI, USA) were used as secondary antibodies for immunoblotting.

2.8. Statistical analysis

Statistical significance was evaluated by unpaired *t*-test. All data are expressed as mean ± SEM. When more than three groups were compared, one-way ANOVA with Fischer's post hoc test was used. $P < 0.05$ was considered to be statistically significant.

3. Results

3.1. Dietary salt regulates ubiquitination of NCC in mouse kidney

In order to investigate whether ubiquitination of NCC is involved in the regulation of its abundance in the kidney, we examined NCC ubiquitination in the kidney from mice under various dietary salt intake conditions. As shown in Fig. 1A, NCC protein abundance and phosphorylation were increased under a low-salt diet and decreased under a high-salt diet, as reported previously [9]. NCC ubiquitination was then evaluated under the same conditions. As shown in Fig. 1A and B, ubiquitination of NCC was significantly elevated and reduced in kidneys from mice fed high-salt and low-salt diets, respectively.

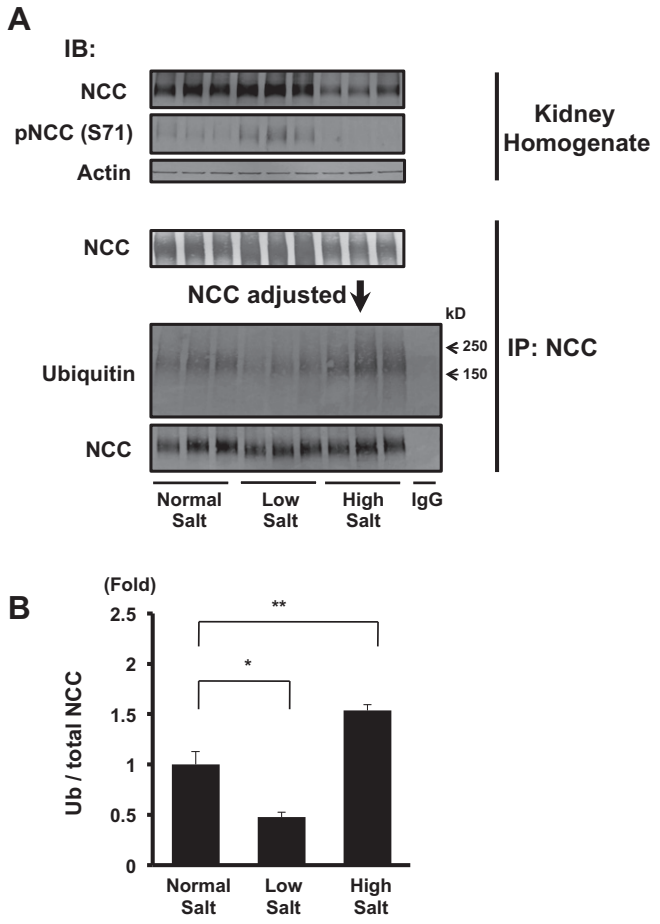

Fig. 1. Ubiquitination of NCC is regulated by dietary salt intake. (A) Immunoblots of total and phosphorylated NCC in the kidneys of wild-type mice fed diets with different amounts of salt. NCC Phosphorylation at S71 was regulated by different amounts of salt in the diet; phosphorylation and abundance of NCC decreased under a high-salt diet and increased under a low-salt diet (upper panels). NCC was immunoprecipitated from kidney homogenates of mice fed diets containing different amounts of salt. Immunoprecipitated NCC was adjusted to have nearly equal amounts of immunoprecipitated NCC in each lane in order to more clearly demonstrate the differences in ubiquitination in each lane (lower panel). Immunoprecipitated NCC was blotted with ubiquitin antibody. NCC ubiquitination was lower in mice fed low-salt diet and higher in mice fed high-salt diet, as compared to mice fed normal diet. (B) Densitometry analysis of ubiquitination of immunoprecipitated NCC in mice fed different amounts of salt. For densitometry analysis, values are expressed as ratios of ubiquitinated and total NCC against mean signals in the normal diet group. $^{**}P < 0.01$, $^{*}P < 0.05$.

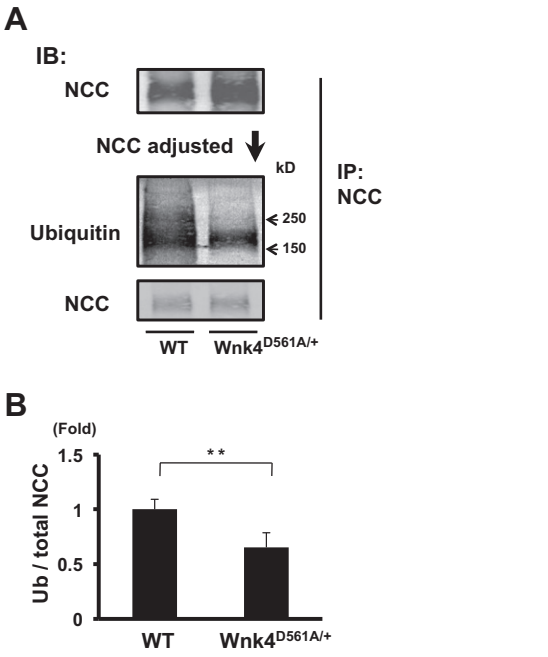

Fig. 2. Ubiquitination of NCC was reduced in *Wnk4*$^{D561A/+}$ mouse kidney. (A) Representing immunoblots of NCC ubiquitination in *Wnk4*$^{D561A/+}$ mouse kidney. NCC was immunoprecipitated from kidney homogenates of *Wnk4*$^{D561A/+}$ mice and their wild-type littermates. Immunoprecipitated NCC was adjusted to have nearly equal amounts of immunoprecipitated NCC in each lane in order to more clearly demonstrate the differences in ubiquitination in each lane. NCC ubiquitination was lower in *Wnk4*$^{D561A/+}$ mice, as compared to their wild-type littermates. (B) Densitometry analysis of NCC ubiquitination in *Wnk4*$^{D561A/+}$ mice. Ubiquitination of NCC in *Wnk4*$^{D561A/+}$ mice was significantly lower, as compared to their wild-type littermates. Values ($n = 5$) are normalized by immunoprecipitated total NCC. $^{**}P < 0.01$.

3.2. Decreased ubiquitination of NCC due to increased phosphorylation is involved in pathogenesis of PHAII

Previously, we generated *Wnk4*$^{D561A/+}$ knock-in mice, a mouse model of PHAII, and found that the pathogenesis of PHAII involves the constitutive activation of the WNK-OSR1/SPAK kinases-NCC phosphorylation cascade, resulting in the gain of NCC function. In this PHAII mouse model, both total and phosphorylated NCC was elevated in the kidney [3]. As observed in the mice fed low-salt diet, NCC was less ubiquitinated in the PHAII model mouse kidney, as compared with wild-type littermates (Fig. 2). These results clearly indicate that increased phosphorylation of NCC by activated WNK-OSR1/SPAK-NCC phosphorylation cascade results in decreased ubiquitination of NCC.

3.3. Phosphorylation of NCC decreased its ubiquitination

In mice, the major sites of NCC phosphorylation by OSR1 and SPAK are Thr 53, Thr 58 and Ser 71 [4]. To clarify the relationship between the phosphorylation of NCC at these sites and NCC ubiquitination, we transfected T7-tagged phospho-deficient and -mimicking mutant NCC along with wild-type NCC into COS7 cells (Fig. 3A), and evaluated the ubiquitination of these mutants. Immunoblots of whole cell lysates revealed that total protein abundance of the phospho-mimicking NCC was significantly higher than wild-type and phospho-deficient NCC, thus suggesting that degradation of the phospho-mimicking NCC is decreased (Fig. 3B and C). Ubiquitination of the phospho-mimicking NCC is less than that of wild-type and the phospho-deficient NCC, and is inversely correlated with total NCC abundance (Fig. 3D). These results clearly indicate that phosphorylation of NCC at Thr 53, Thr 58 and Ser 71 decreases NCC ubiquitination, and as a result, increases NCC protein abundance. It has been reported that NCC exhibits distinctive bands on immunoblots that correspond to molecular masses of 95, 110, 130 to 140 and more than 250 kDa [24,25]. Nonglycosylated 95 kDa NCC is the core NCC while the 110-kDa band is sensitive to Endo H digestion, corresponding to the endoplasmic reticulum-and/or pre-Golgi complex-retained NCC protein [24]. The glycosylated protein of 130–140 kDa is not sensitive to Endo H digestion and is present in the plasma membrane [24], forming functional homodimer complexes of 250–350 kDa [25]. In Fig. 3, the bands at 110, 130 and 250 kDa were all increased in the phospho-mimicking NCC, indicating that both NCC in the plasma membranes and in intracellular organelles is increased. We detected the smear-like ubiquitinated NCC band extending from about 120 to more than 250 kDa, thus suggesting that NCC ubiquitination in both ER/pre-Golgi and plasma membranes was decreased in the phospho-mimicking NCC.

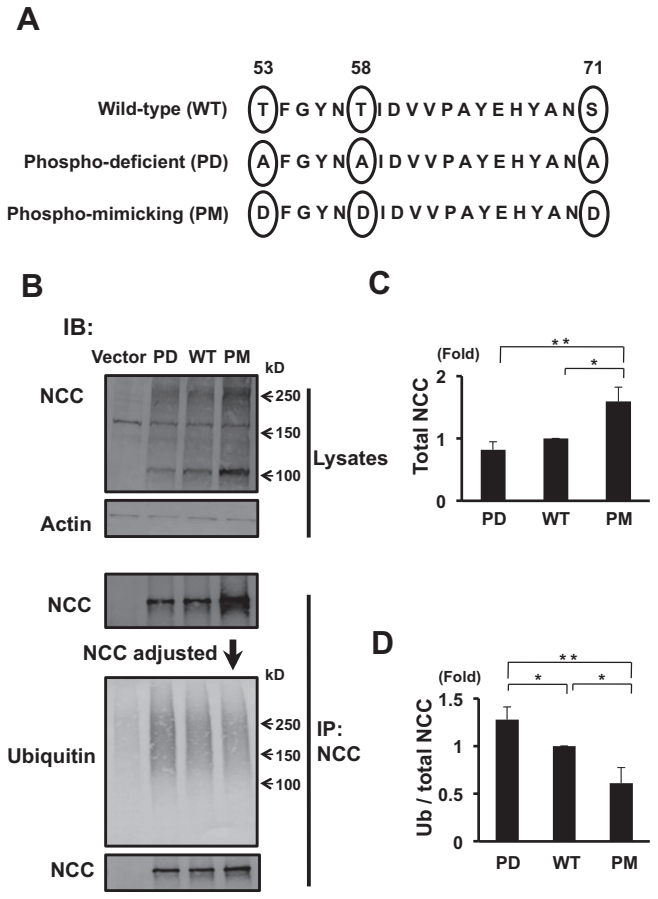

Fig. 3. NCC Phosphorylation increases total expression and decreases ubiquitination in COS7 cells. (A) Three consensus amino-terminal residues (T53, T58 and S71) are critical for the phosphorylation of NCC. In phospho-deficient NCC (PD), these residues are mutated to alanine. In phospho-mimicking NCC (PM), these residues are mutated to aspartic acid. (B) Representative immunoblots of expression and ubiquitination of phospho-deficient, wild-type or phospho-mimicking NCC. Empty vector (Vector), phospho-deficient, wild-type or phospho-mimicking T7-tagged NCC were transfected into COS7 cells. In total cell lysates, expression levels of phospho-mimicking NCC were higher than those of phospho-deficient and wild-type NCC (upper panel). NCC was immunoprecipitated from whole cell lysates, and immunoprecipitated NCC was adjusted to have nearly equal amounts of immunoprecipitated NCC in each lane in order to more clearly demonstrate the differences in ubiquitination in each lane (lower panels). Phospho-mimicking NCC is less ubiquitinated, as compared to phospho-deficient NCC. (C) Densitometry analysis of expression levels of phospho-deficient, wild-type and phospho-mimicking NCC in COS7 cells. Expression levels of phospho-mimicking NCC were significantly higher than those of phospho-deficient and wild-type NCC. For densitometry analysis, values ($n = 4$) are expressed as ratios against mean signals in wild-type NCC. $^{**}P < 0.01$, $^{*}P < 0.05$. (D) Densitometry analysis of ubiquitination of immunoprecipitated NCC from COS7 cells. NCC ubiquitination was corrected against NCC abundance. Phospho-mimicking NCC was significantly less ubiquitinated, as compared to wild-type and phospho-deficient NCC. Wild-type NCC was also less ubiquitinated than phospho-deficient NCC. For densitometry analysis, values ($n = 4$) are expressed as ratios against the mean signals in wild-type NCC. $^{**}P < 0.01$, $^{*}P < 0.05$.

3.4. Phosphorylation of NCC regulates its ubiquitination at the cell surface and increases membrane abundance

Ubiquitination is known to regulate cell surface abundance of ion channels and transporters [26]. Therefore, we examined the effects of NCC phosphorylation on the plasma membrane abundance of NCC, and also evaluated whether phosphorylation decreased NCC ubiquitination within the plasma membranes using the biotin–neutravidin system. Immunoblots of biotinylated cell surface protein with NCC antibody revealed that the cell surface expression of the phospho-mimicking NCC was much higher when compared with wild-type and phospho-deficient NCC (Fig. 4A and B). Biotinylated NCC exhibited bands at more than 250 kDa, indicating that our biotin assay detected NCC only in the plasma membranes. To evaluate the inhibitory effects of NCC phosphorylation on ubiquitination in plasma membranes, we isolated biotinylated surface NCC from COS7 cells by immunoprecipitation with NCC antibody, followed by NeutrAvidin pull down. As shown in Fig. 4C and D, the phospho-mimicking NCC in the plasma membranes showed less ubiquitination than wild-type and phospho-deficient NCC, indicating that the NCC phosphorylation decreases its ubiquitination within plasma membranes.

4. Discussion

The kidney plays an important role in linking salt intake with blood pressure. This vital function is regulated by sodium reabsorption through several ion-transporters expressed along the nephron. NCC plays a major role in renal electrolyte balance. Many

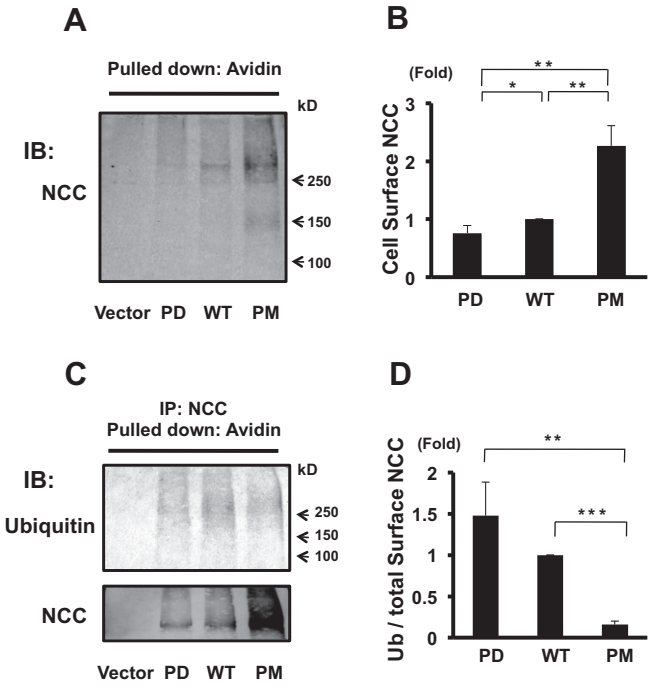

Fig. 4. NCC phosphorylation decreases its ubiquitination within plasma membranes. (A) Representative immunoblot of cell surface expression of phospho-deficient (PD), wild-type (WT) or phospho-mimicking (PM) NCC. COS7 cells were transfected with empty vector, PD, WT or PM T7-tagged NCC. Cell surface proteins were pulled down with biotinylation-neutravidin assay and blotted with anti-T7 antibody. (B) Densitometry analysis of surface NCC expression. Surface expression of phospho-mimicking NCC was also significantly higher than that of phospho-deficient and wild-type NCC. Surface expression of wild-type NCC was significantly higher than that of phospho-deficient NCC. For densitometry analysis, values are expressed as ratios against mean signals in wild-type NCC. $^{**}P < 0.01$, $^{*}P < 0.05$. (C) Representative blots of ubiquitination of biotinylated NCC. COS7 cells were transfected with empty vector, phospho-deficient (PD), wild-type (WT) or phospho-mimicking (PM) T7-tagged NCC. After cell surface biotinylation, NCC was immunoprecipitated by rabbit anti-NCC antibody. Immunoprecipitated and biotinylated NCC were pulled down with NeutrAvidin and blotted with ubiquitin and T7 antibody. In this experiment, immunoprecipitated-biotinylated NCC was not adjusted, as available samples in this assay were insufficient to be re-loaded. (D) Densitometry analysis of ubiquitination of immunoprecipitated NCC at the cell surface. Ubiquitination of phospho-mimicking NCC at the cell surface was much less than that of phospho-deficient and wild-type NCC. Ubiquitination of wild-type NCC was also less than that of phospho-deficient NCC, indicating that phosphorylation of NCC decreases its ubiquitination at the cell surface. For densitometry analysis, values ($n = 3$) are normalized against immunoprecipitated surface total NCC and are expressed as ratios against mean signals in wild-type NCC. $^{***}P < 0.001$ $^{**}P < 0.01$.

reports have shown that phosphorylation of NCC plays an essential role in NCC function [3–6,27,28]. In addition, total NCC abundance in the kidney appears to vary according to NCC phosphorylation status. However, it remains to be determined how the phosphorylation of NCC regulates its total protein abundance in the kidney. In this study, we clarified the role of phosphorylation on NCC abundance by focusing on NCC ubiquitination. We found that total protein abundance of the phospho-mimicking NCC in COS7 cells was significantly increased, as compared to phospho-deficient and wild-type NCC. Moreover, ubiquitination of phospho-mimicking NCC is lower than that of wild-type and phospho-deficient NCC, and inversely correlated with abundance (Fig. 3). These results clearly indicate that either phosphorylation of NCC inhibits or dephosphorylation of NCC promotes NCC ubiquitination, thereby regulating NCC abundance within cells.

This notion was supported by the *in vivo* evidence, i.e., the decreased NCC ubiquitination in *Wnk4*$^{D561A/+}$ knock-in PHAII model mice, where increased NCC phosphorylation and total protein abundance were observed in the kidney. As the mRNA of NCC was not increased in this PHAII mouse model (data not shown), it was clear that the degradation pathway of NCC played a key role in increased protein abundance. In addition to the PHAII mouse model, we also confirmed in wild-type mice that the increased and decreased phosphorylation of NCC by different salt diets decreased and increased NCC ubiquitination, respectively. Based on these data, we concluded that the ubiquitination of NCC is a major mechanism for regulating NCC protein abundance in kidney following changes in NCC phosphorylation.

In addition to total NCC protein abundance within cells, plasma membrane localization is important for NCC function *in vivo* [3]. Ubiquitination regulates a number of cell surface proteins by stimulating their internalization from the cell surface [26]. It was previously shown that NCC phosphorylated at Thr 53, Thr 58 and Ser 71 accumulated in the apical membranes of DCT, thus suggesting that phosphorylation of NCC is important for plasma membrane localization [7,8]. However, the underlying mechanism(s) remain to be determined. In our biotinylation assay, we demonstrated that phosphorylation of NCC regulates surface expression as observed in the *in vivo* kidney. Furthermore, we found that the phospho-mimicking NCC showed less ubiquitination within the plasma membranes (Fig. 4), thus suggesting that the phosphorylated NCC in the plasma membranes is less ubiquitinated, thereby increasing NCC abundance in plasma membranes. Although there have been several reports on the ubiquitination of NCC [18,19], further investigations will be required to clarify the detailed mechanism(s) of how phosphorylation of NCC affects the ubiquitination of NCC.

In summary, we demonstrated that NCC phosphorylation increased plasma membrane localization of NCC and decreased NCC ubiquitination. Decreased ubiquitination may be a major mechanism for accumulation of phosphorylated NCC in the plasma membranes.

Acknowledgments

This study was supported in part by Grants-in-Aid for Scientific Research (A) and for Scientific Research on Innovative Areas from the Japan Society for the Promotion of Science, Grant-in-Aid for Young Scientists (B) from the Ministry of Education, Culture, Sports, Science and Technology of Japan, Salt Science Research Foundation (No. 1228), Takeda Science Foundation, and The Nakajima Foundation.

References

[1] D.B. Simon, C. Nelson-Williams, M.J. Bia, D. Ellison, F.E. Karet, A.M. Molina, I. Vaara, F. Iwata, H.M. Cushner, M. Koolen, F.J. Gainza, H.J. Gitleman, R.P. Lifton, Gitelman's variant of Bartter's syndrome, inherited hypokalaemic alkalosis, is caused by mutations in the thiazide-sensitive Na–Cl cotransporter, Nat. Genet. 12 (1996) 24–30.

[2] F.H. Wilson, S. Disse-Nicodème, K.A. Choate, K. Ishikawa, C. Nelson-Williams, I. Desitter, M. Gunel, D.V. Milford, G.W. Lipkin, J.M. Achard, M.P. Feely, B. Dussol, Y. Berland, R.J. Unwin, H. Mayan, D.B. Simon, Z. Farfel, X. Jeunemaitre, R.P. Lifton, Human hypertension caused by mutations in WNK kinases, Science 293 (2001) 1107–1112.

[3] S.S. Yang, T. Morimoto, T. Rai, M. Chiga, E. Sohara, M. Ohno, K. Uchida, S.H. Lin, T. Moriguchi, H. Shibuya, Y. Kondo, S. Sasaki, S. Uchida, Molecular pathogenesis of pseudohypoaldosteronism type II: generation and analysis of a Wnk4(D561A/+) knockin mouse model, Cell Metab. 5 (2007) 331–344.

[4] C. Richardson, D.R. Alessi, The regulation of salt transport and blood pressure by the WNK-SPAK/OSR1 signalling pathway, J. Cell Sci. 121 (2008) 3293–3304.

[5] S.S. Yang, Y.F. Lo, C.C. Wu, S.W. Lin, C.J. Yeh, P. Chu, H.K. Sytwu, S. Uchida, S. Sasaki, S.H. Lin, SPAK-knockout mice manifest Gitelman syndrome and impaired vasoconstriction, J. Am. Soc. Nephrol. 21 (2010) 1868–1877.

[6] D. Pacheco-Alvarez, P.S. Cristóbal, P. Meade, E. Moreno, N. Vazquez, E. Muñoz, A. Díaz, M.E. Juárez, I. Giménez, G. Gamba, The Na^+:Cl^- cotransporter is activated and phosphorylated at the amino-terminal domain upon intracellular chloride depletion, J. Biol. Chem. 281 (2006) 28755–28763.

[7] N.B. Pedersen, M.V. Hofmeister, L.L. Rosenbaek, J. Nielsen, R.A. Fenton, Vasopressin induces phosphorylation of the thiazide-sensitive sodium chloride cotransporter in the distal convoluted tubule, Kidney Int. 78 (2010) 160–169.

[8] K. Mutig, T. Saritas, S. Uchida, T. Kahl, T. Borowski, A. Paliege, A. Böhlick, M. Bleich, Q. Shan, S. Bachmann, Short-term stimulation of the thiazide-sensitive Na^+–Cl^- cotransporter by vasopressin involves phosphorylation and membrane translocation, Am. J. Physiol. Renal Physiol. 298 (2010) F502–509.

[9] M. Chiga, T. Rai, S.S. Yang, A. Ohta, T. Takizawa, S. Sasaki, S. Uchida, Dietary salt regulates the phosphorylation of OSR1/SPAK kinases and the sodium chloride cotransporter through aldosterone, Kidney Int. 74 (2008) 1403–1409.

[10] G. Talati, A. Ohta, T. Rai, E. Sohara, S. Naito, A. Vandewalle, S. Sasaki, S. Uchida, Effect of angiotensin II on the WNK-OSR1/SPAK-NCC phosphorylation cascade in cultured mpkDCT cells and in vivo mouse kidney, Biochem. Biophys. Res. Commun. 393 (2010) 844–848.

[11] M.B. Sandberg, A.D. Riquier, K. Pihakaski-Maunsbach, A.A. McDonough, A.B. Maunsbach, ANG II provokes acute trafficking of distal tubule Na^+–Cl(−) cotransporter to apical membrane, Am. J. Physiol. Renal Physiol. 293 (2007) F662–669.

[12] P. San-Cristobal, D. Pacheco-Alvarez, C. Richardson, A.M. Ring, N. Vazquez, F.H. Rafiqi, D. Chari, K.T. Kahle, Q. Leng, N.A. Bobadilla, S.C. Hebert, D.R. Alessi, R.P. Lifton, G. Gamba, Angiotensin II signaling increases activity of the renal Na–Cl cotransporter through a WNK4-SPAK-dependent pathway, Proc. Natl. Acad. Sci. USA 106 (2009) 4384–4389.

[13] E. Sohara, T. Rai, S.S. Yang, A. Ohta, S. Naito, M. Chiga, N. Nomura, S.H. Lin, A. Vandewalle, E. Ohta, S. Sasaki, S. Uchida, Acute insulin stimulation induces phosphorylation of the Na–Cl cotransporter in cultured distal mpkDCT cells and mouse kidney, PLoS One 6 (2011) e24277.

[14] F.H. Rafiqi, A.M. Zuber, M. Glover, C. Richardson, S. Fleming, S. Jovanović, A. Jovanović, K.M. O'Shaughnessy, D.R. Alessi, Role of the WNK-activated SPAK kinase in regulating blood pressure, EMBO Mol. Med. 2 (2010) 63–75.

[15] R. Zhou, S.V. Patel, P.M. Snyder, Nedd4-2 catalyzes ubiquitination and degradation of cell surface ENaC, J. Biol. Chem. 282 (2007) 20207–20212.

[16] L. Schild, Y. Lu, I. Gautschi, E. Schneeberger, R.P. Lifton, B.C. Rossier, Identification of a PY motif in the epithelial Na channel subunits as a target sequence for mutations causing channel activation found in Liddle syndrome, EMBO J. 15 (1996) 2381–2387.

[17] K.K. Knight, D.R. Olson, R. Zhou, P.M. Snyder, Liddle's syndrome mutations increase Na^+ transport through dual effects on epithelial Na^+ channel surface expression and proteolytic cleavage, Proc. Natl. Acad. Sci. USA 103 (2006) 2805–2808.

[18] P.G. Needham, K. Mikoluk, P. Dhakarwal, S. Khadem, A.C. Snyder, A.R. Subramanya, J.L. Brodsky, The thiazide-sensitive NaCl cotransporter is targeted for chaperone-dependent endoplasmic reticulum-associated degradation, J. Biol. Chem. 286 (2011) 43611–43621.

[19] J.P. Arroyo, D. Lagnaz, C. Ronzaud, N. Vázquez, B.S. Ko, L. Moddes, D. Ruffieux-Daidié, P. Hausel, R. Koesters, B. Yang, J.B. Stokes, R.S. Hoover, G. Gamba, O. Staub, Nedd4-2 modulates renal Na^+–Cl^- cotransporter via the aldosterone-SGK1-Nedd4-2 pathway, J. Am. Soc. Nephrol. 22 (2011) 1707–1719.

[20] T. Moriguchi, S. Urushiyama, N. Hisamoto, S. Iemura, S. Uchida, T. Natsume, K. Matsumoto, H. Shibuya, WNK1 regulates phosphorylation of cation-chloride-coupled cotransporters via the STE20-related kinases, SPAK and OSR1, J. Biol. Chem. 280 (2005) 42685–42693.

[21] K. Susa, S. Kita, T. Iwamoto, S.S. Yang, S.H. Lin, A. Ohta, E. Sohara, T. Rai, S. Sasaki, D.R. Alessi, S. Uchida, Effect of heterozygous deletion of WNK1 on the WNK-OSR1/SPAK-NCC/NKCC1/NKCC2 signal cascade in the kidney and blood vessels, Clin. Exp. Nephrol. (2012).

[22] K. Oi, E. Sohara, T. Rai, M. Misawa, M. Chiga, D.R. Alessi, S. Sasaki, S. Uchida, A minor role of WNK3 in regulating phosphorylation of renal NKCC2 and NCC co-transporters in vivo, Biol. Open 1 (2011) 120–127.

[23] A. Ohta, T. Rai, N. Yui, M. Chiga, S.S. Yang, S.H. Lin, E. Sohara, S. Sasaki, S. Uchida, Targeted disruption of the Wnk4 gene decreases phosphorylation of Na–Cl cotransporter, increases Na excretion and lowers blood pressure, Hum. Mol. Genet. 18 (2009) 3978–3986.

[24] J.C. De Jong, W.A. Van Der Vliet, L.P. Van Den Heuvel, P.H. Willems, N.V. Knoers, R.J. Bindels, Functional expression of mutations in the human NaCl cotransporter: evidence for impaired routing mechanisms in Gitelman's syndrome, J. Am. Soc. Nephrol. 13 (2002) 1442–1448.
[25] J.C. de Jong, P.H. Willems, F.J. Mooren, L.P. van den Heuvel, N.V. Knoers, R.J. Bindels, The structural unit of the thiazide-sensitive NaCl cotransporter is a homodimer, J. Biol. Chem. 278 (2003) 24302–24307.
[26] L. Hicke, R. Dunn, Regulation of membrane protein transport by ubiquitin and ubiquitin-binding proteins, Annu. Rev. Cell Dev. Biol. 19 (2003) 141–172.
[27] S. Uchida, Pathophysiological roles of WNK kinases in the kidney, Pflugers Arch. 460 (2010) 695–702.
[28] J.A. McCormick, J.H. Nelson, C.L. Yang, J.N. Curry, D.H. Ellison, Overexpression of the sodium chloride cotransporter is not sufficient to cause familial hyperkalemic hypertension, Hypertension 58 (2011) 888–894.